Draft version February 3, 2023
Typeset using LaTeX **preprint** style in AASTeX63

PROVABGS Early Data Release: Probabilistic Stellar Mass Function

ChangHoon Hahn[1,*]
[1] *Department of Astrophysical Sciences, Princeton University, Peyton Hall, Princeton NJ 08544, USA*

(Dated: `DRAFT -- 6d00025 -- 2021-01-14 -- NOT READY FOR DISTRIBUTION`)

ABSTRACT

Keywords: keyword1 – keyword2 – keyword3

1. INTRODUCTION

2. THE DESI BRIGHT GALAXY SURVEY EARLY DATA RELEASE

brief description of the DESI BGS early data release and fuji reduction

We focus on BGS galaxies at $z < 0.3$.

3. PROVABGS SED MODELING

For each BGS EDR galaxy, we derive its M_* and other properties, $\overline{\rm SFR}$, $Z_{\rm MW}$, and $t_{\rm age,MW}$ from DESI photometry and spectroscopy using the PROVABGS SED modeling framework (Hahn et al. 2022). PROVABGS models galaxy SEDs using stellar population synthesis with non-parametric star-formation history (SFH) with a starburst, a non-parametric metallicity history (ZH) that varies with time, and a flexible dust attenuation prescription. The non-parameteric SFH and ZH prescriptions are derived from SFHs and ZHs of simulated galaxies in the Illustris hydrodynamic simulation (Vogelsberger et al. 2014; Genel et al. 2014; Nelson et al. 2015) and provide compact and flexibly representations of SFHs and ZHs. For the stellar population synthesis, PROVABGS uses the Flexible Stellar Population Synthesis (FSPS; Conroy et al. 2009, 2010) model with MIST isochrones (Paxton et al. 2011, 2013, 2015; Choi et al. 2016; Dotter 2016), Chabrier (2003) initial mass function (IMF), and a combination of MILES (Sánchez-Blázquez et al. 2006) and BaSeL (Lejeune et al. 1997, 1998; Westera et al. 2002) spectral libraries.

Furthermore, PROVABGS provides a Bayesian inference framework for inferring full posterior probability distributions of the SED model parameter: $p(\theta\,|\,\mathbf{X}^{\rm photo}, \mathbf{X}^{\rm spec})$, where $\mathbf{X}^{\rm photo}$ represents the photometry and $\mathbf{X}^{\rm spec}$ represents the spectroscopy. In total, θ has 13 parameters: M_*, 6 parameters specifying the SFH ($\beta_1, \beta_2, \beta_3, \beta_4, f_{\rm burst}, t_{\rm burst}$), 2 parameters specifying ZH (γ_1, γ_2), 3 parameters specifying dust attenuation ($\tau_{\rm BC}, \tau_{\rm ISM}, n_{\rm dust}$), and a nuisance parameter for the fiber aperture effect. Posteriors have distinct advantages over point estimates because they accurately estimate uncertainties and degeneracies among galaxy properties. Furthermore, as we later demonstrate, they are essential for principled population inference: *e.g.* SMF.

* changhoon.hahn@princeton.edu

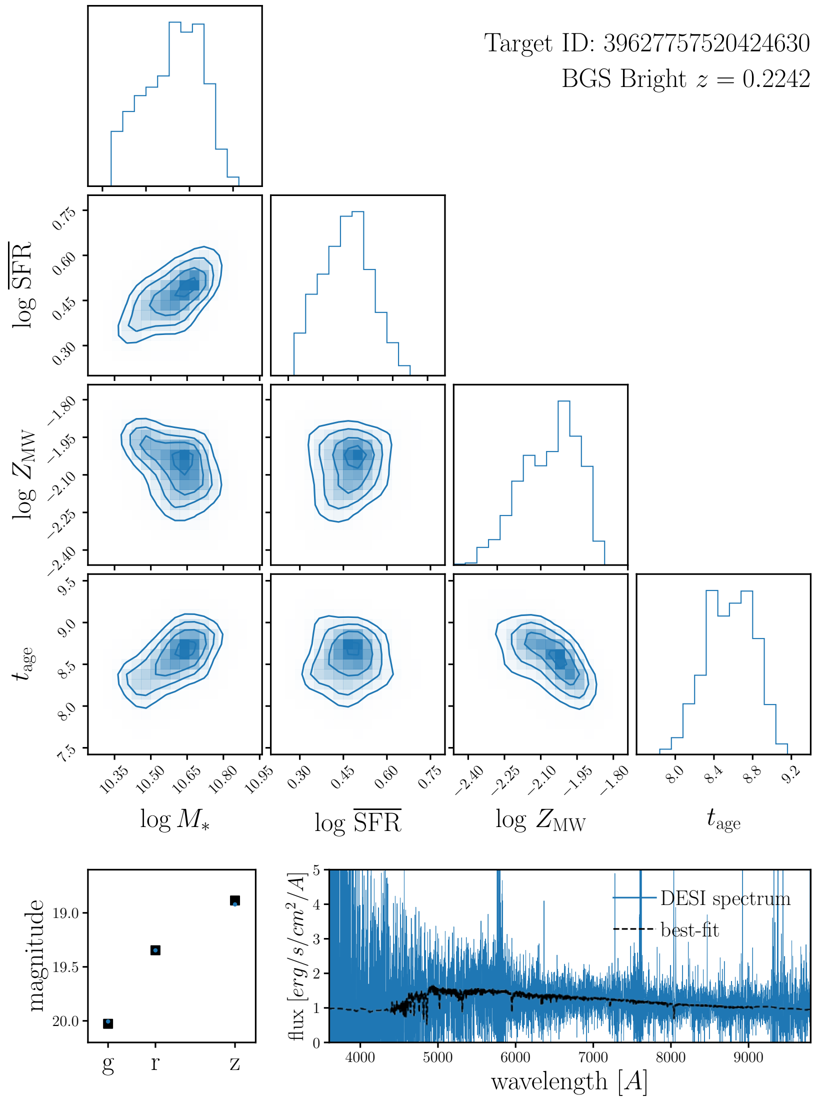

Figure 1.

In practice, accurately estimating a 13 dimensional posterior requires a large number ($\gtrsim$100,000) SED model evaluations, which would require prohibitive computational resources. To address this challenge, PROVABGS samples the posterior using the Karamanis & Beutler (2020) ensemble slice Markov Chain Monte Carlo (MCMC) sampling with the ZEUS Python package[1]. PROVABGS further accelerates the inference by using neural emulators for the SED models. The emulators are accurate to subpercent level and $>100\times$ faster than the original SED model based on FSPS (Kwon et al. 2022). With ZEUS and neural emulation, deriving a posterior takes $\sim$5 min per galaxy with PROVABGS. Moreover, Hahn et al. (2022) demonstrated PROVABGS can accurately infer M_* overall the full expected M_* range of BGS, using forward modeled synthetic DESI observations.

In Figure 1,

[1] https://zeus-mcmc.readthedocs.io/

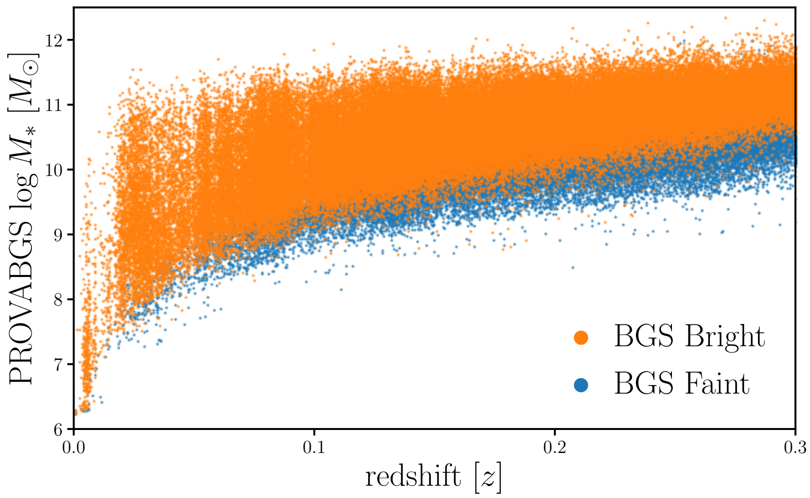

Figure 2.

Figure 2,

4. RESULTS

We are interested in estimating the SMF of BGS galaxies from their individual marginalized posteriors, $p(M_* \,|\, \boldsymbol{X}_i)$, derived using PROVABGS (Section 3).

we're going to do population inference in a hierarchical bayesian framework and use a normalizing flow.

why? because it produces unbiased inference.

why do we use normalizing flows?

We follow the same approach as Hahn et al. (2022) to estimate:

$$p(\phi \,|\, \{\boldsymbol{X}_i\}) = \frac{p(\phi)\; p(\{\boldsymbol{X}_i\} \,|\, \phi)}{p(\{\boldsymbol{X}_i\})} \tag{1}$$

$$= \frac{p(\phi)}{p(\{\boldsymbol{X}_i\})} \int p(\{\boldsymbol{X}_i\} \,|\, \{\theta_i\})\; p(\{\theta_i\} \,|\, \phi)\; \mathrm{d}\{\theta_i\}. \tag{2}$$

$$= \frac{p(\phi)}{p(\{\boldsymbol{X}_i\})} \prod_{i=1}^{N} \int p(\boldsymbol{X}_i \,|\, \theta_i)\; p(\theta_i \,|\, \phi)\; \mathrm{d}\theta_i \tag{3}$$

$$= \frac{p(\phi)}{p(\{\boldsymbol{X}_i\})} \prod_{i=1}^{N} \int \frac{p(\theta_i \,|\, \boldsymbol{X}_i)\; p(\boldsymbol{X}_i)}{p(\theta_i)}\; p(\theta_i \,|\, \phi)\; \mathrm{d}\theta_i \tag{4}$$

$$= p(\phi) \prod_{i=1}^{N} \int \frac{p(\theta_i \,|\, \boldsymbol{X}_i)\; p(\theta_i \,|\, \phi)}{p(\theta_i)}\; \mathrm{d}\theta_i. \tag{5}$$

We estimate the integral using S_i Monte Carlo samples from the individual posteriors $p(\theta_i \,|\, \boldsymbol{X}_i)$:

$$\approx p(\phi) \prod_{i=1}^{N} \frac{1}{S_i} \sum_{j=1}^{S_i} \frac{p(\theta_{i,j} \,|\, \phi)}{p(\theta_{i,j})}. \tag{6}$$

BGS provides two samples: BGS Bright and Faint. Galaxies in BGS Bright are selected based on a $r < 19.5$ flux limit, while the ones in BGS Faint are selected based on a fiber-magnitude and color limit and $r < 20.0175$ flux limit. Since neither of these samples are volume-limited and complete as a function of M_*, we must include the selection effect when estimating the SMF. We do this by including weights derived from $z^{\rm max}$, the maximum redshift that galaxy i could be placed and still be included in the BGS samples. We derive $z_i^{\rm max}$ for every galaxy using by redshifting the SED predicted by the best-fit parameters. We then derive $V_i^{\rm max}$, the comoving volume out to $z_i^{\rm max}$, and weights $w_i = w_{i,{\rm comp}}/V_i^{\rm max}$. We modify Eq. 1 to include w_i:

$$p(\phi \,|\, \{\boldsymbol{X}_i\}) \approx \frac{p(\phi)}{\prod\limits_{i=1}^{N} p(\boldsymbol{X}_i)^{w_i}} \prod_{i=1}^{N} \left(\int p(\boldsymbol{X}_i \,|\, \theta_i)\; p(\theta_i \,|\, \phi)\; {\rm d}\theta_i \right)^{w_i} \tag{7}$$

$$\approx \frac{p(\phi)}{\prod\limits_{i=1}^{N} p(\boldsymbol{X}_i)^{w_i}} \prod_{i=1}^{N} \left(\sum_{j=1}^{S_i} \frac{p(\theta_{i,j} \,|\, \phi)}{p(\theta_{i,j})} \right)^{w_i} \tag{8}$$

$$\approx \frac{p(\phi)}{\prod\limits_{i=1}^{N} p(\boldsymbol{X}_i)^{w_i}} \prod_{i=1}^{N} \left(\sum_{j=1}^{S_i} \frac{q_\phi(\theta_{i,j})}{p(\theta_{i,j})} \right)^{w_i}. \tag{9}$$

In practice, we do not derive the full posterior $p(\phi \,|\, \{\boldsymbol{X}_i\})$. Instead we derive the maximum a posteriori (MAP) hyperparameter $\phi_{\rm MAP}$ that maximizes $p(\phi \,|\, \{\boldsymbol{X}_i\})$ or $\log p(\phi \,|\, \{\boldsymbol{X}_i\})$. We expand,

$$\log p(\phi \,|\, \{\boldsymbol{X}_i\}) \approx \log p(\phi) + \sum_{i=1}^{N} w_i \log \left(\sum_{j=1}^{S_i} \frac{q_\phi(\theta_{i,j})}{p(\theta_{i,j})} \right). \tag{10}$$

Since the first two terms are constant, we derive $\phi_{\rm MAP}$ by maximizing

$$\max_{\phi} \quad \sum_{i=1}^{N} w_i \log \left(\sum_{j=1}^{S_i} \frac{q_\phi(\theta_{i,j})}{p(\theta_{i,j})} \right). \tag{11}$$

We use Adam optimizer and determine the architecture of the normalizing flow through experimentation.

4.1. *The Probabilistic Stellar Mass Function*

ACKNOWLEDGEMENTS

It's a pleasure to thank

APPENDIX

A. SPECTROSCOPIC COMPLETENESS

fiber assignment completeness: weights available from the alternate MTLs

redshift failure weights based on TSNR2 and fiber flux

B. STELLAR MASS COMPLETENESS

First, we take galaxies with $i\Delta z < z < (i+1)\Delta z$.

For each galaxy take their best-fit SED from PROVABGS and artificially redshift it to $z' = z + \Delta z$.

afterward, calculate the r band magnitude using the best-fit SED and determine whether the galaxy at z' would be within the target selection.

We then compare the M_* distributions and determine the M_* below which a significant number of galaxies are excluded from the sample.

REFERENCES

Chabrier G., 2003, Publications of the Astronomical Society of the Pacific, 115, 763

Choi J., Dotter A., Conroy C., Cantiello M., Paxton B., Johnson B. D., 2016, The Astrophysical Journal, 823, 102

Conroy C., Gunn J. E., White M., 2009, The Astrophysical Journal, 699, 486

Conroy C., White M., Gunn J. E., 2010, The Astrophysical Journal, 708, 58

Dotter A., 2016, The Astrophysical Journal Supplement Series, 222, 8

Genel S., et al., 2014, Monthly Notices of the Royal Astronomical Society, 445, 175

Hahn C., et al., 2022, The DESI PRObabilistic Value-Added Bright Galaxy Survey (PROVABGS) Mock Challenge

Karamanis M., Beutler F., 2020, arXiv e-prints, p. arXiv:2002.06212

Kwon K. J., Hahn C., Alsing J., 2022, Neural Stellar Population Synthesis Emulator for the DESI PROVABGS

Lejeune T., Cuisinier F., Buser R., 1997, A & A Supplement series, Vol. 125, October II 1997, p.229-246., 125, 229

Lejeune T., Cuisinier F., Buser R., 1998, Astronomy and Astrophysics Supplement, v.130, p.65-75, 130, 65

Nelson D., et al., 2015, Astronomy and Computing, 13, 12

Paxton B., Bildsten L., Dotter A., Herwig F., Lesaffre P., Timmes F., 2011, The Astrophysical Journal Supplement Series, 192, 3

Paxton B., et al., 2013, The Astrophysical Journal Supplement Series, 208, 4

Paxton B., et al., 2015, The Astrophysical Journal Supplement Series, 220, 15

Sánchez-Blázquez P., et al., 2006, Monthly Notices of the Royal Astronomical Society, 371, 703

Vogelsberger M., et al., 2014, Monthly Notices of the Royal Astronomical Society, 444, 1518

Westera P., Lejeune T., Buser R., Cuisinier F., Bruzual G., 2002, Astronomy and Astrophysics, 381, 524